



The Particular Expression Profiles of Circular RNA in Peripheral Blood of Myocardial Infarction Patients by RNA Sequencing

Qi Li^{1,2,3†}, Yuanyong Wang^{4†}, Yi An⁵, Jianxun Wang^{3*} and Yufang Gao^{6*}

¹ School of Nursing, Qingdao University, Qingdao, China, ² Department of Nursing, The Affiliated Hospital of Qingdao University, Qingdao, China, ³ School of Basic Medical Sciences, Qingdao University, Qingdao, China, ⁴ Department of Thoracic Surgery, Tangdu Hospital of Air Force Military Medical University, Xi'an, China, ⁵ Department of Cardiology, The Affiliated Hospital of Qingdao University, Qingdao, China, ⁶ Department of Emergency, The Affiliated Hospital of Qingdao University, Qingdao, China

OPEN ACCESS

Edited by:

Ramcés Falfán-Valencia,
Instituto Nacional de Enfermedades
Respiratorias-México (INER), Mexico

Reviewed by:

Thasni Karedath,
Qatar Biomedical Research Institute,
Qatar
David Cruz Robles,
National Cardiology Institute Ignacio
Chavez, Mexico

*Correspondence:

Yufang Gao
gaoyufang0612@163.com
Jianxun Wang
wangjx@qdu.edu.cn

† These authors have contributed
equally to this work

Specialty section:

This article was submitted to
Cardiovascular Genetics and Systems
Medicine,
a section of the journal
Frontiers in Cardiovascular Medicine

Received: 06 November 2021

Accepted: 10 May 2022

Published: 06 June 2022

Citation:

Li Q, Wang Y, An Y, Wang J and
Gao Y (2022) The Particular
Expression Profiles of Circular RNA
in Peripheral Blood of Myocardial
Infarction Patients by RNA
Sequencing.
Front. Cardiovasc. Med. 9:810257.
doi: 10.3389/fcvm.2022.810257

Myocardial infarction (MI) is one of the most common illnesses seriously harmful to human health. Notwithstanding, the systems of its pathogenesis are as yet not totally demonstrated. CircRNA is one sort of non-coding RNA, and late distributed information proposes that circRNAs assume a significant part in heart diseases; however, their expression profiles in the peripheral blood of patients with MI are not yet totally characterized. Therefore, RNAs from peripheral blood were recruited for high-throughput RNA-seq analysis. A total of 3,862 circRNAs were distinguished to be remarkably different, including 2,738 circRNAs being upregulated and 1,124 circRNAs being downregulated. circTMEM165, circUBAC2, circZNF609, circANKRD12, and circSLC8A1 were reconfirmed by RT-qPCR in the cell model. ROC curves uncovered that they have great sensitivity and specificity in the determination of MI. Besides, circRNAs are associated with cell metabolism and function by directing complex networks among circular RNAs, microRNAs, and messenger RNAs. In outline, our study portrayed the specific articulation profiles of circular RNA in patients with MI. The outcomes showed that circRNAs might fill in as a sort of ideal biomarkers for MI diagnosis. Further exploration of these circRNAs may enrich our understanding of MI etiology and progression.

Keywords: circular RNA, myocardial infarction, RNA sequencing, biomarkers, cardiovascular diseases

INTRODUCTION

Cardiovascular diseases (CVDs) are the most common cause of death globally. The number of deaths from CVD accounted for about one-third of all global deaths (1). Myocardial infarction (MI) is the most common diseases in CVDs and has the highest fatality rate (2, 3). Around 85% of deaths in CVDs are owing to MI and stroke. MI is a multifactorial disease, which involved in complex

Abbreviations: MI, myocardial infarction; circRNA, circular RNA; RT-qPCR, real-time quantitative polymerase chain reaction; ROC, receiver operating characteristic; GO, Gene Ontology; KEGG, Kyoto Encyclopedia of Genes and Genomes; miRNA, microRNA; CVDs, cardiovascular diseases; RNA-Seq, high-throughput RNA sequencing; EDTA, ethylenediaminetetraacetic acid; qPCR, quantitative PCR; AUC, the area under the curve; ROS, reactive oxygen species; BP, biological process; CC, cellular component; MF, molecular function; LDL, low-density lipoprotein; CAD, artery disease.

pathogenesis (4). MI is instigated by partial or complete blockage of the coronary artery (5). The consequence of blocked coronary arteries is an ischemic injury to the region of the heart (6). Once the myocardial cell is damaged by ischemia, dead cardiomyocytes, instead of fibroblasts, ultimately resulted in remodeling, ventricular malfunction, chronic heart failure, and even sudden cardiac death (7–11). It is generally believed that myocardial ischemia is irreversible after 12 h of MI, which is the key factor to impact on patient prognosis (5). Hence, seeking inchoate and accurate biomarkers of MI is urgently needed to improve diagnostic efficiency and the health of the public.

Recently, circRNAs have become the focus and the front field of RNA research based on advanced RNA sequencing technology and bioinformatics analysis. circRNA is a kind of non-coding RNA, which contains a closed continuous loop structure and is broadly expressed in multispecies genomes (12, 13). circRNAs were first revealed years ago, but their functions in cells are freshly appreciating and developing recently (14). Most researchers reported that circRNAs are responsible for regulating gene expression principally by binding with and then resulting in miRNAs dysfunction (9). Ongoing exploration has uncovered that circRNAs work as contending endogenous RNAs or miRNA wipes, as target-RNA decoys by binding to RBPs (15), as regulators of transcription and splicing by binding srnRNA and upgrading Pol II activities (16), and as protein scaffolds (17) and modifiers of parental gene expression. A recent study confirms that circRNAs are a key factor in CVDs (18). Abnormally expressed circRNAs were strongly linked to the occurrence and progress of CVDs, for instance, MI (9), hypertrophy, heart failure (19), and atherosclerosis (20), indicating the potential effects of circRNA in CVDs. Taken together, a lot of evidence affords a novel orientation for discovering circRNAs as a new-fashioned biomarker for the diagnosis of CVDs.

The peripheral blood involves numerous leukocyte subpopulations, for instance, T cells, B cells, mononuclear cells, and natural killer cells. Studies have shown that key genes in leukocytes are associated with alterations in gene expression and the onset of disease (21).

To date, the associations between circRNAs in peripheral blood and MI are not fully understood. Therefore, we explored the expression profiles of circRNA in patients with MI and healthy controls by high-throughput circRNA sequencing. We collected the volunteers' peripheral blood and constructed the cell model to confirm the dysregulated circRNAs. ROC and combined ROC curves were created for demonstrating the biomarkers of MI. The roles of circRNAs in MI were analyzed by bioinformatics. Moreover, we discovered a possible complex endogenic RNA regulatory network among circRNAs-miRNAs-mRNAs, with a view to providing some references for related research in this field.

MATERIALS AND METHODS

All testing programs were performed according to the protocols approved by the Medical Ethics Committee of the Affiliated Hospital of Qingdao University. All sample providers were

informed of their blood samples, clinical data were used for this study, and informed consents were signed.

Sample Collection

The peripheral blood samples from 80 patients with MI were collected before percutaneous coronary intervention surgery between March 2018 and January 2019 in the Affiliated Hospital of Qingdao University (19). All patients were not treated with heparin, radiotherapy, or chemotherapy. The matched healthy controls were collected from the volunteers of the physical examination center (**Supplementary Table 4**). Fresh peripheral blood samples (5 ml) from patients with MI and healthy individuals were collected in EDTA tubes.

Total RNA Extraction

The samples were used for RNA extraction *via* the TRIzol method (Trizol-up reagents, TransGen, China). This experiment was performed according to the kit's recommendations. RNA samples were stored at -80°C .

RNA Quantification and Qualification

The purity of the extracted RNA was tested by a NanoPhotometer® Spectrophotometer (IMPLEN, CA, United States). RNA concentration was detected by Qubit® RNA Assay Kit in Qubit® 2.0 Fluorometer (Life Technologies, CA, United States). RNA integrity was measured by the RNA Nano 6000 Assay Kit of the Bioanalyzer 2100 system (Agilent Technologies, CA, United States). RNA degradation and contamination were monitored on 1% agarose gels.

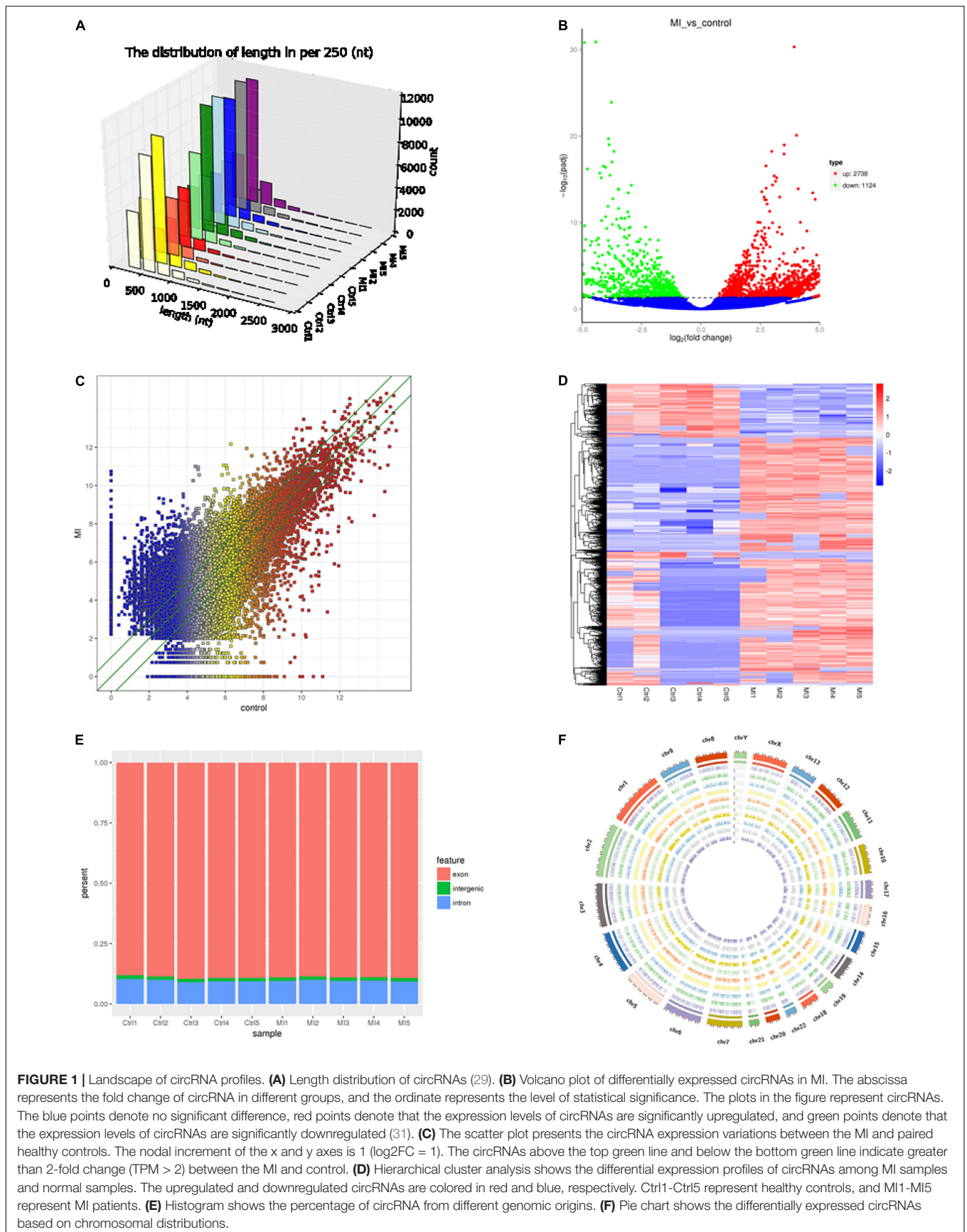
Library Preparation and circRNA Sequencing

A total of 5 μg RNA per sample was used for the RNA library preparations. First, rRNA was removed by Epicenter Ribozero™ rRNA Removal Kit (Epicenter, United States) and ethanol precipitation. Subsequently, the linear RNA was digested with RNaseR (Epicenter, United States). The sequencing libraries were produced by NEBNext® Ultra™ Directional RNA Library Prep Kit for Illumina® (NEB, United States).

The cluster generation of the index-coded samples was performed on a cBot Cluster Generation System using TruSeq PE Cluster Kit v3-cBot-HS. After that, the libraries were sequenced on an Illumina HiSeq 4000 platform. These experiments were performed following the manufacturer's instructions.

Data Analysis and circRNA Identification

First, clean data were gained by wiping off reads containing adapter and low-quality reads from raw data. The clean data with high quality were used for downstream analyses. Index of the reference genome was created using Bowtie2 v2.2.8, and paired-end clean reads were united to the reference genome using Bowtie (22). The circRNAs were detected and verified by using *find_circ* (23) and CIRI2 (24). The Circos software was used to construct the circos figure.



Divergent Polymerase Chain Reaction

The junction site part of circRNAs was confirmed by polymerase chain reaction (PCR) with divergent primers. Convergent primers were used as the control. The products of the PCR amplification were authenticated by 1% agarose gel electrophoresis. The primers for circRNA validation are listed in **Supplementary Table 1**.

Real-Time Quantitative Polymerase Chain Reaction

The dysregulation circRNA was reconfirmed on a CFX96 Real-Time PCR Detection System (Bio-Rad). Total RNA was extracted using Trizol reagent. Reverse transcription reactions were performed by using the TransScript II One-Step gDNA Removal and cDNA Synthesis SuperMix (TransGen, China) to make cDNA according to the manufacturer's guide. TransStart Green qPCR SuperMix (TransGen) was used for quantitative PCR (qPCR) analysis, and the procedures were performed in accordance with the kit instructions. The levels of dysregulation circRNA analyzed by RT-qPCR were normalized to that of GAPDH (21). The primers for RT-qPCR are listed in **Supplementary Table 2**.

Creation of Receiver Operating Characteristic Curves

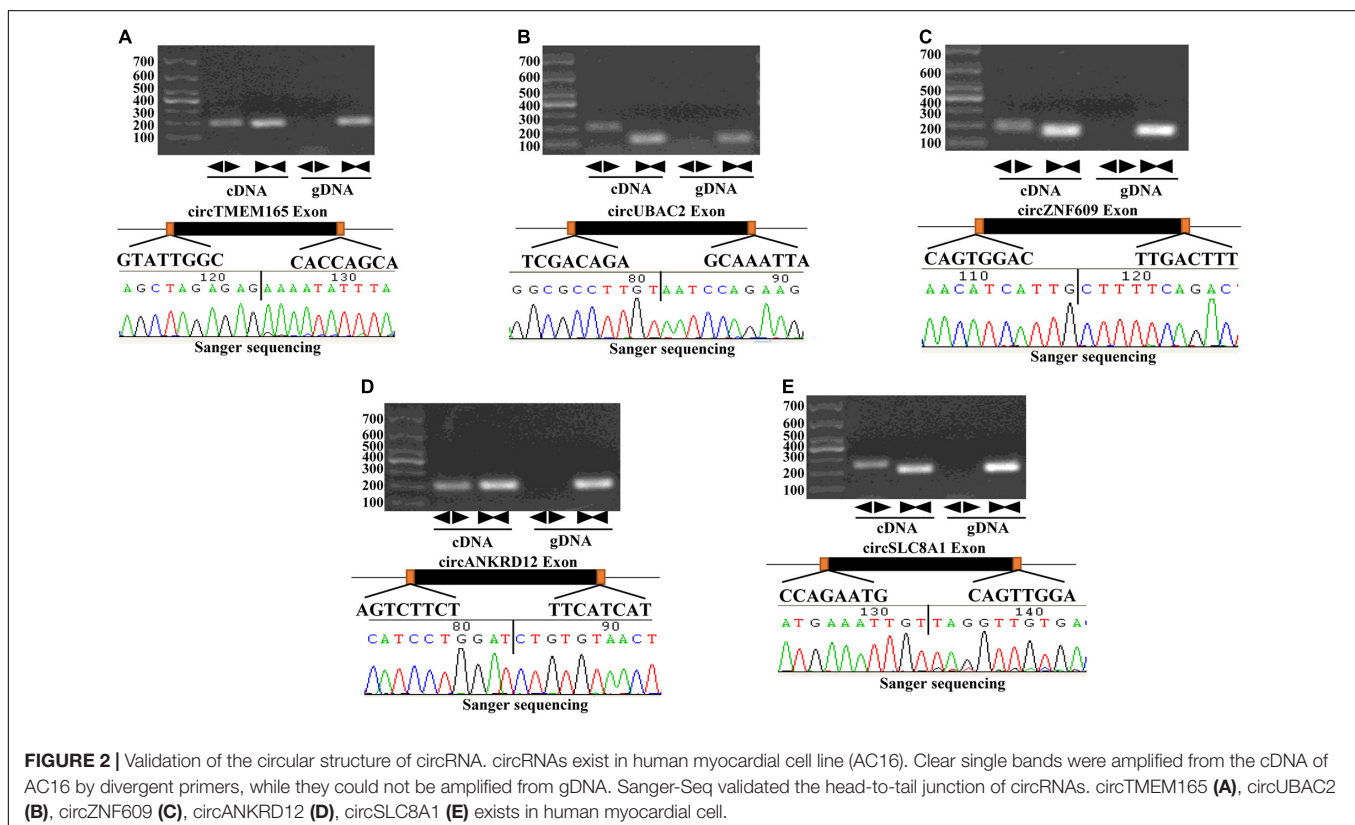
The ROC curves were created to estimate the diagnostic value of circRNAs for MI. An ROC curve was calculated, and the

specificity and sensitivity of predictive power were measured by the AUC. The AUC was used to assess the diagnostic value of the circRNAs in the peripheral blood of patients with MI (25). The combination ROC is made by the combined predictors obtained by the regression of the five genes of interest. SPSS26.0 and Graphpad prism7 were used for calculating and drawing the ROC curve.

Gene Ontology and Kyoto Encyclopedia of Genes and Genomes Enrichment Analysis

Gene Ontology (GO) enrichment analysis for host genes of differentially expressed circRNAs was carried out by the GO seq R package, and the gene length bias was corrected during this procedure (26). GO terms with corrected *P*-value less than 0.05 were considered to be significantly enriched by differential expressed genes. As a database resource for understanding high-level functions and utilities of the biological system (27), Kyoto Encyclopedia of Genes and Genomes (KEGG) is used to explore information from the molecular level (such as the cell, the organism, and the ecosystem), especially large-scale molecular datasets generated by genome sequencing and other high-throughput experimental technologies.¹ We used the KOBAS software to test the statistical enrichment of differential expression genes or circRNA host genes in KEGG pathways (28).

¹<http://www.genome.jp/kegg/>



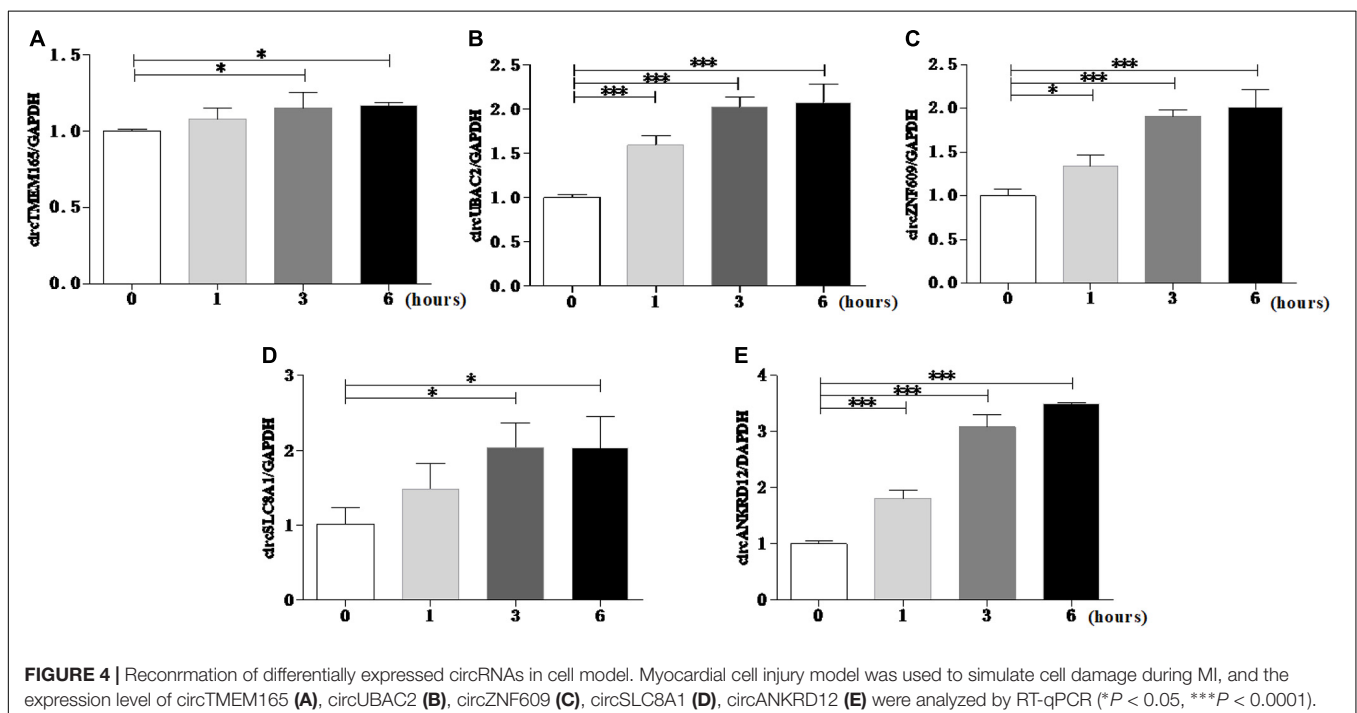
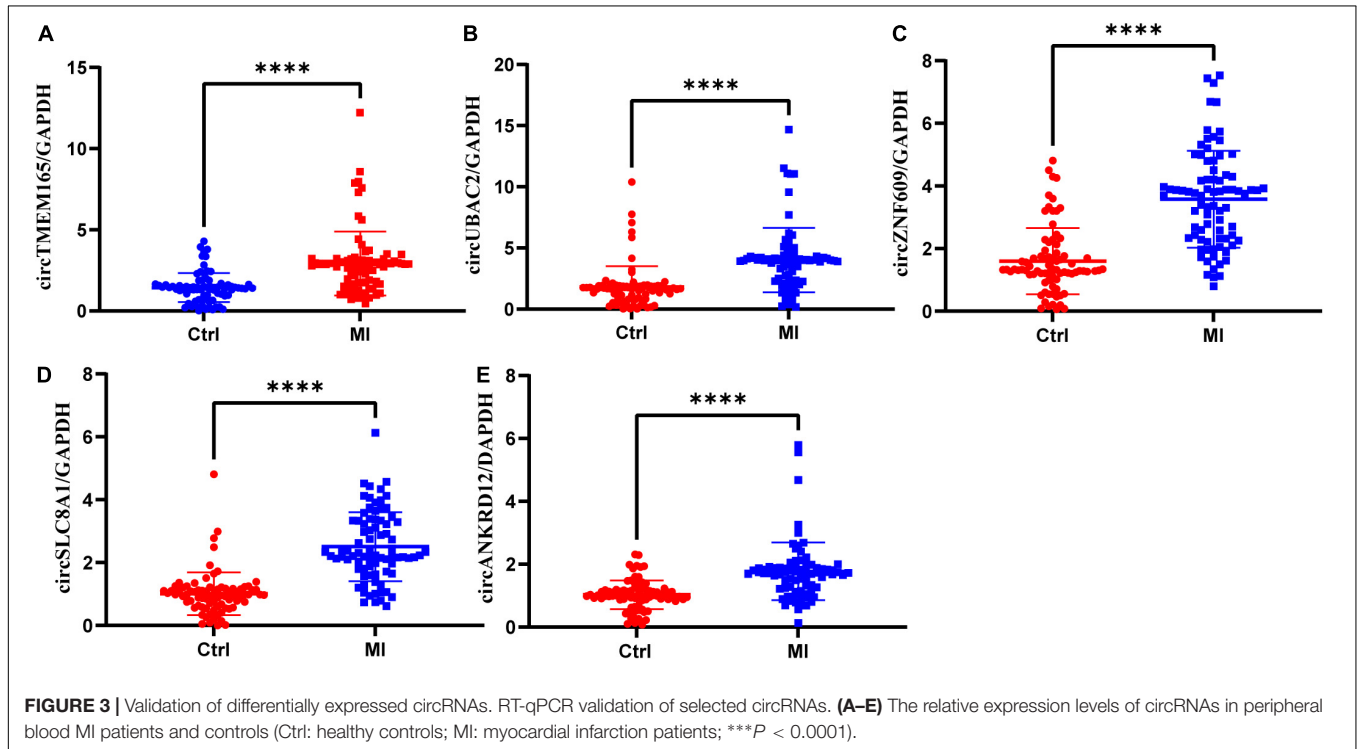
Prediction of the Network of circRNAs-MiRNAs-mRNAs

circRNA can regulate the translation of mRNA *via* binding to an miRNA (9). miRNA target sites in the exons of circRNA loci were verified by using miRanda. The binding sites of miRNA and mRNA were predicted by RNAhybrid.

Cytoscape was used to construct the circRNA-miRNA-mRNA networks.

Cell Culture and Treatment

AC16 cells were cultured in DMEM (Gibco) with 10% fetal bovine serum (TransGen), and 100 U/ml penicillin and



100 mg/ml streptomycin (Invitrogen) in a humidified 5% CO₂ incubator at 37°C. When the cultured cells reached approximately 70% confluent, they were treated with H₂O₂ (100 μM and 500 μM, respectively) incubated at 37°C for 12 h in a complete culture medium. The cells were collected for RNA extraction and dysregulated circRNA reconfirmation.

Apoptosis Assays

Apoptosis was determined by the terminal deoxynucleotidyl transferase-mediated dUTP nick-end labeling (TUNEL) using a kit from TransGen. The detection procedures were in accordance with the kit instructions.

Mitochondrial Staining and Analysis of Mitochondrial Fission

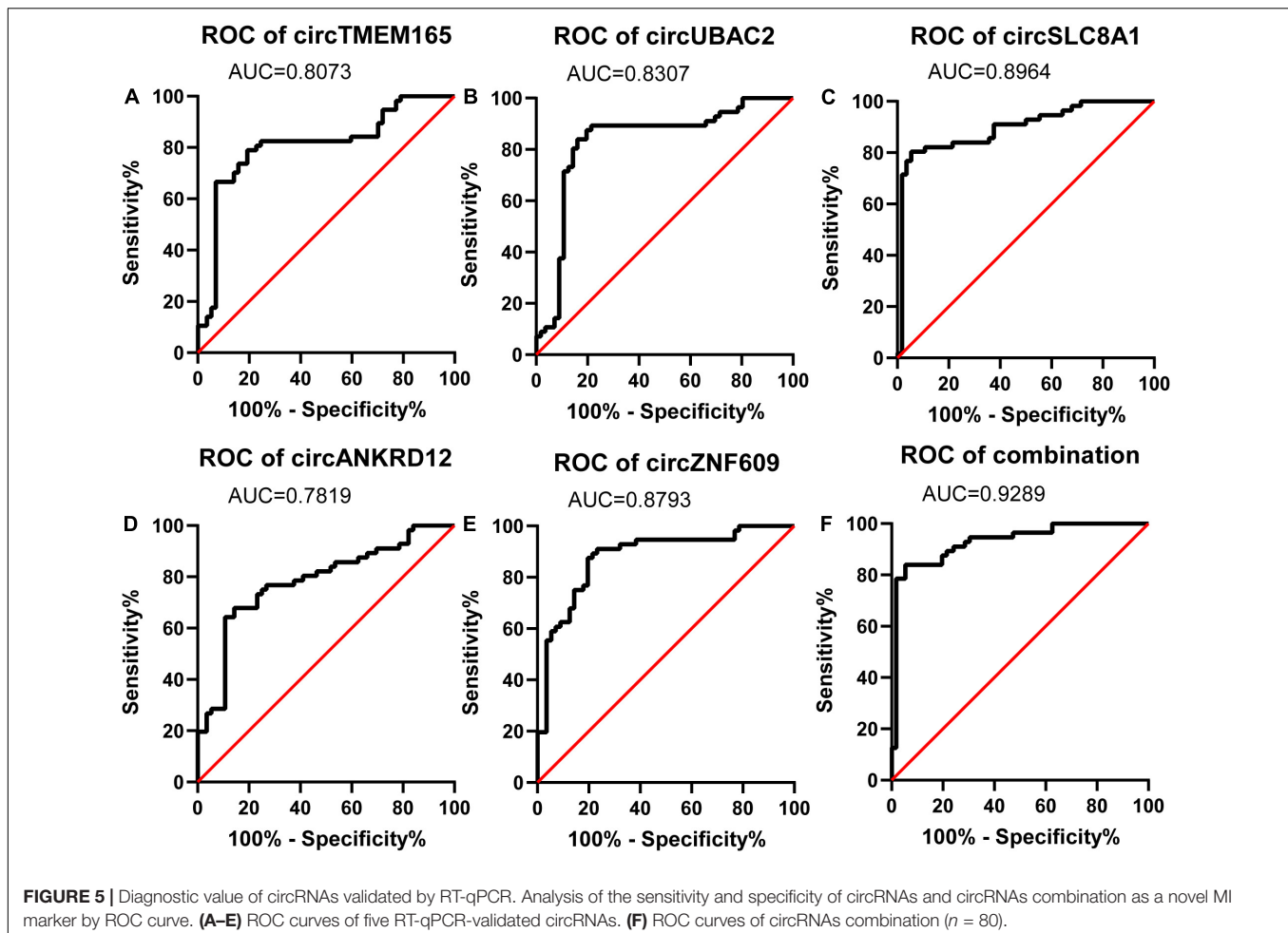
Mitochondrial staining was performed as described earlier with modifications (29). Briefly, cells were plated onto the poly-L-lysine-coated coverslips. After treatment, they were stained for 30 min with 0.02 μM MitoTracker Red at 37°C. Mitochondria were imaged using a laser-scanning confocal microscope (Zeiss LSM510 META).

Immunoblotting

Immunoblot was carried out as described earlier (30). Briefly, the cells were lysed for 20 min on ice in RIPA lysis buffer containing a protease inhibitor cocktail and DMSF. The samples were subjected to 12% SDS-PAGE and transferred to nitrocellulose membranes. Blots were probed with primary antibodies anti-Caspase-3 (Abcom, 1:1,000), anti-Cyto c (Abclone, 1:1,000), anti-Tublin (Affinity, 2:1,000), and anti-β-actin (TransGen, 1:2,000) at 4°C overnight with gently shaking. After three times washing with PBS, the horseradish peroxidase (HRP)-conjugated secondary antibodies were added. Antigen-antibody complexes were visualized by enhanced chemiluminescence. Enhanced ECL™ prime detection reagent (30) was used to visualize antigen-antibody complexes, and the density was quantified by ImageJ.

Statistical Analysis

The results are expressed as mean ± SEM of at least three independent experiments. The statistical comparison between different groups was completed by one-way ANOVA for multiple comparisons or *t*-test with Welch's correction for two groups. Statistical analyses were completed with GraphPad Prism 7.0



(GraphPad Software, Inc., San Diego, CA). $P < 0.05$ was regarded as statistically significant.

RESULTS

The Landscape of circRNA Expression Profiles in Peripheral Blood From Patients With Myocardial Infarction and Healthy Individuals

The circRNAs were identified by find_circ and Bowtie2 based on the high-quality clean data. A total of 3,862 circRNAs were recognized in five pairs of MI and healthy controls samples. The size of the circRNAs extended from ≈ 100 to 2,500 nt (Figure 1A). The differentially expressed circRNAs were analyzed by DEGseq, and the results were considered statistically significant when $\text{padj} < 0.05$. The differentially expressed profiles of circRNAs among the two groups are shown in Figures 1B,C. Hierarchical clustering heatmap analysis shown in Figure 1D illustrates a unique circRNA expression landscape among the MI and healthy individuals. Our results presented that there was an obvious difference in circRNA expression profile between the MI and healthy controls. Consequently, 3,862 circRNAs were altered in the patients with MI. In total, 2,738 circRNAs were upregulated and 1,124 circRNAs were downregulated in the MI group compared with the healthy controls. Of the distinguishably expressed circRNAs, 89% are exonic, 10% are intronic, and 1% are intergenic (Figure 1E). As shown in Figure 1F, the transcription of dysregulated circRNAs was observed to be broadly dispersed in all chromosomes, and chr1, chr2, chr3, chr4, chr5, chr6, chr7, chr8, chrX, and chr9 are the top ten circRNAs. The top 50 differentially expressed circRNAs are depicted in Supplementary Table 2.

CircRNAs Screening and Circle Structure Identification

First, we screened candidate circRNAs by comparing our results with the previous study on human heart tissue sequencing sample results (Supplementary Figure 1) (31) in order to improve the accuracy of our research. Then, we detected the circle structure of intersection circRNAs. We tested the expression of intersection circRNAs by adding them to the cDNA of myocardial cells by using the divergent primer (Supplementary Table 1). Additionally, the added products of circRNAs were sequenced by using Sanger sequencing to further confirm the circularized junction size of the circRNAs (Figure 2).

Authentication of Differentially Expressed circRNAs

To verify the RNA-seq data, five intersectional circRNAs (i.e., circTMEM165, circUBAC2, circZNF609, circANKRD12, and circSLC8A1) were selected and validated by RT-qPCR using 80 MI samples and 80 healthy individuals. The general information of selected circRNAs shown as Table 1. The results revealed that the expression of these five circRNAs was upregulated in patients

with MI (Figure 3). The RT-qPCR data were strongly consistent with the circRNA sequencing results.

To reconfirm the dysregulation of these circRNAs in the cell model, we used the myocardial cell injury model induced by reactive oxygen species (ROS) to simulate cell damage during MI (9). The data of the cell model showed that all the validated circRNAs were upregulated with prolonged stimulation time (Figure 4). This result was consistent with the data on peripheral blood. Collectively, these two results verified the accuracy and repeatability of the circRNA sequencing results.

The Potential Diagnostic Values of circRNAs for Patients With Myocardial Infarction

To evaluate the potential diagnostic value of selected circRNAs for MI, we computed and created ROC curves (Figure 5) for RT-qPCR-validated circRNAs to discriminate patients with MI from healthy individuals according to the fold changes of these circRNAs' expression. We trained the model with 70% of the samples and validated it with the remaining 30% of the data (Supplementary Figure 2).

The calculated optimal cutoff point for circTMEM165 level in the peripheral blood was 1.6089505 (Youden index = 0.55), while the sensitivity and specificity were 21.3% and 23.7%, respectively. The calculated optimal cutoff point for circUBAC2 level was 1.968652 (Youden index = 0.663), while the sensitivity and specificity were 82.5% and 83.8%, respectively. The calculated optimal cutoff point for circ ZNF609 level was 1.947015 (Youden index = 0.638), while the sensitivity and specificity were 86.3% and 77.5%, respectively. The calculated optimal cutoff point for circ SLC8A1 level was 1.5414885 (Youden index = 0.737), while the sensitivity and specificity were 82.5% and 91.25%, respectively. The calculated optimal cutoff point for circANKRD12 level was 1.4872795 (Youden index = 0.575), while

TABLE 1 | The general information of circRNA.

circBase_ID	Gene name	MI_readcount	Control_readcount
hsa_circ_0000826	ANKRD12	816.599493	79.5731602
hsa_circ_0001414	TMEM165	720.396765	102.724399
hsa_circ_0000615	ZNF609	509.23034	0
hsa_circ_0030720	UBAC2	328.578223	24.0160633
hsa_circ_0000994	SLC8A1	313.178477	0

TABLE 2 | AUC of RT-qPCR-validated circRNAs in patients' validation.

circRNA	Validation patients (n = 50)		
	AUC	95% Confidence interval	P value
circTMEM165	0.8073	0.7225 to 0.8921	< 0.0001
circUBAC2	0.8307	0.7466 to 0.9147	< 0.0001
circZNF609	0.8793	0.8136 to 0.9450	< 0.0001
circSLC8A1	0.8964	0.8345 to 0.9583	< 0.0001
circANKRD12	0.7819	0.6950 to 0.8688	< 0.0001
circRNAs combination	0.9289	0.8793 to 0.9784	< 0.0001

the sensitivity and specificity were 87.5% and 57.5%, respectively. The optimal cutoff point of the combination was 0.06, while the sensitivity, specificity, and Youden index were 0.863, 0.937, and 0.8, respectively. The results revealed that the AUC of these circRNAs at least reached 0.8073, and the AUC of recombination circRNAs reached up to 0.9289 (Table 2), indicating that these circRNAs expressed in peripheral blood could set apart the patients with MI from the healthy individuals. Our data discovered the potential values of circRNAs MI diagnosis.

Enrichment Analysis of circRNAs Host Genes

The source genes of the validated differentially expressed circRNAs were uncovered by using GO annotation, as shown in Figure 6A. The most remarkably improved GO terms about the biological process (BP), cellular component (CC), and molecular function (MF) classes were cellular macromolecule metabolic process (GO:0044260, $P = 2.892E-46$), intracellular

part (GO:0044424, $P = 5.136E-69$), and protein binding (GO:0005515, $P = 8.9672E-34$), respectively.

The data of the KEGG pathway study of the circRNAs genes are shown in Figure 6B. The most relevant genes of differentially expressed circRNAs are ubiquitin-mediated proteolysis (rich factor = 0.328467153, q-value = 1.56E-06, gene number = 45).

Predicted circRNA-miRNA-mRNA Regulatory Network

The miRNA binding sites exist in circRNAs, which can function as miRNA sponges. To further explore their possible roles in patients with MI, we predicted the circRNA-miRNA-mRNA network and analyzed using miRanda and RNAhybrid. The top five predicted miRNAs for these upregulated circRNAs are shown in Table 3, and the target mRNAs of miRNAs are listed in Supplementary Table 3. Additionally, circRNA-miRNA-targeted mRNA networks are also constructed for showing regulatory relationships between them (Figure 7).

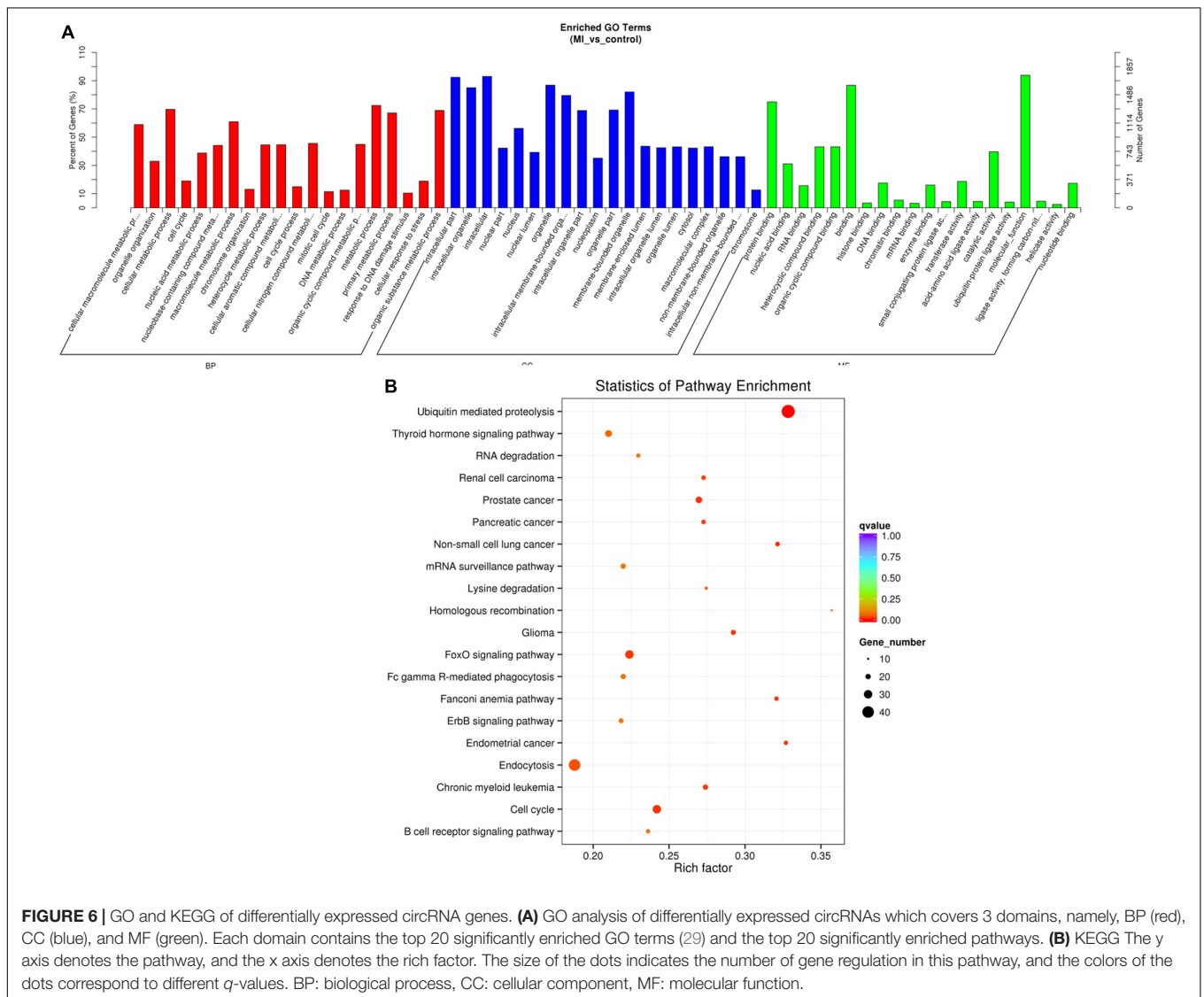


TABLE 3 | The predicted miRNAs related to circRNAs.

Upregulated circRNAs	Predicted miRNAs
circTMEM165	hsa-miR-103b
	hsa-miR-1255b-2-3p
	hsa-miR-1323
	hsa-miR-548a-3p
	hsa-miR-1251-5p
circUBAC2	hsa-miR-200b-3p
	hsa-miR-2115-5p
	hsa-miR-509-5p
	hsa-miR-519d-5p
	hsa-miR-539-3p
circZNF609	hsa-miR-644a
	hsa-miR-4303
	hsa-miR-221-5p
	hsa-miR-1260b
	hsa-miR-1247-5p
circSLC8A1	hsa-miR-1202
	hsa-miR-27a-3p
	hsa-miR-27b-3p
	hsa-miR-30d-3p
	hsa-miR-628-5p
circANKRD12	hsa-miR-876-5p
	hsa-miR-452-3p
	hsa-miR-3167
	hsa-miR-143-3p
	hsa-miR-130b-5p

Moreover, we noted the potential function of these regulatory networks. For example, circTMEM165 is predicted as “sponge” to hsa-miR-548a-3p, which can bind to mRNA GREM1, which is responsible for regulating organogenesis, body patterning, and tissue differentiation. The network of circZNF609-hsa-miR-221-5p-WDR7 may be involved in the low-density lipoprotein (LDL) metabolism. The regulatory pathway of circANKRD12-hsa-miR-876-5p-MYLK may promote myosin interaction with actin and facilitate to produce contractile activity. circANKRD12-hsa-miR-130b-5p targets both ACSM2A and RNF213, which regulate mitochondrial acyl-coenzyme A synthetase and ATPase activity, respectively. These networks indicate the possible interactional RNA regulatory relationships between circRNAs, miRNAs, and mRNAs in MI.

Knockdown circSLC8A1 Reduced Myocardial Cell to Apoptosis Under Oxidative Stress

As circSLC8A1 has the best ROC in the verification of clinical samples, we should further explore its mechanism of action in MI. To further clarify the underlying mechanism of circSLC8A1 in MI, we first knocked down circSLC8A1 expression in the myocardial cells through circSLC8A1-siRNA. The AC16 cells were treated with 100 μ M H₂O₂ after the knockdown of circSLC8A1 expression. We found that the number of apoptotic cells was significantly decreased in the si-circSLC8A1 group (Figures 8A,B), and the percentage of

fragmented mitochondrial cells were significantly reduced in the siRNA group compared with other groups (Figures 8C,D). To investigate whether circSLC8A1 is involved in mitochondrial apoptosis, we detected the expression level of apoptosis-related proteins *via* Western blot analysis, and our results revealed that the expression levels of Caspase3 and cyto c were markedly decreased (Figures 8E,F). These data revealed that under slight oxidative stress, cell apoptosis was more hard induced after the knockdown of circSLC8A1.

Taken together, these data demonstrated that knockdown of circSLC8A1 decreased intracellular oxidative stress, kept the balance of mitochondria dynamics, and then reduced apoptosis during oxidative stress.

Overexpression of circSLC8A1 Sensitized Myocardial Cell to Apoptosis Under Oxidative Stress

To understand the role of circSLC8A1 in myocardial cell apoptosis, we overexpressed circSLC8A1 in AC16 cells using circSLC8A1-plasmid. After transfection, the cell was treated with 100 μ M H₂O₂. The results indicated that overexpression of circSLC8A1 remarkably promotes mitochondria fission (Figure 9C), and the percentage of fragmented mitochondrial cells were significantly increased (Figure 9D). In cell apoptosis assays, we found that the proportion of TUNEL-positive cells was raised compared with the related controls (Figures 9A,B). We also examined the expression level of apoptosis-associated proteins by Western blot assay; the results showed that in the circSLC8A1 OE group, the expression levels of Caspase3 and cyto c were significantly increased (Figures 9E,F).

Altogether, our results demonstrated that the overexpression of circSLC8A1 increased the intracellular oxidative stress, and it sensitized the myocardial cells to apoptosis by further increasing mitochondrial fission under the stimulation of oxidative stress.

DISCUSSION

Myocardial infarction is a kind of multifactorial disease, which causes complex pathogenesis and leads to high mortality. It is hard to diagnose and prompt the intervention of MI before the disease occurs. As a consequence, there is an earnest for early detection markers for MI diagnosis. circRNAs are single-stranded, covalently closed molecules (32) that are expressed in numerous species (23, 33). The application of cutting-edge RNA-seq innovation has improved our understanding of knowledge about the specific circRNA expression profiles in human diseases (12). Some researchers pointed out that circRNAs may serve as a novel kind of ideal biomarker for disease diagnosis (34). In this study, circRNA-seq was employed to distinguish differences in the expression profiles of circRNA in peripheral blood between patients with MI and healthy individuals, and our results revealed the possible contribution of differentially expressed circRNAs in MI pathology.

Recent reports have demonstrated that circRNAs are more constant, varied, and conserved when compared with other kinds of RNAs, including mRNAs, miRNAs, and lncRNAs (23).

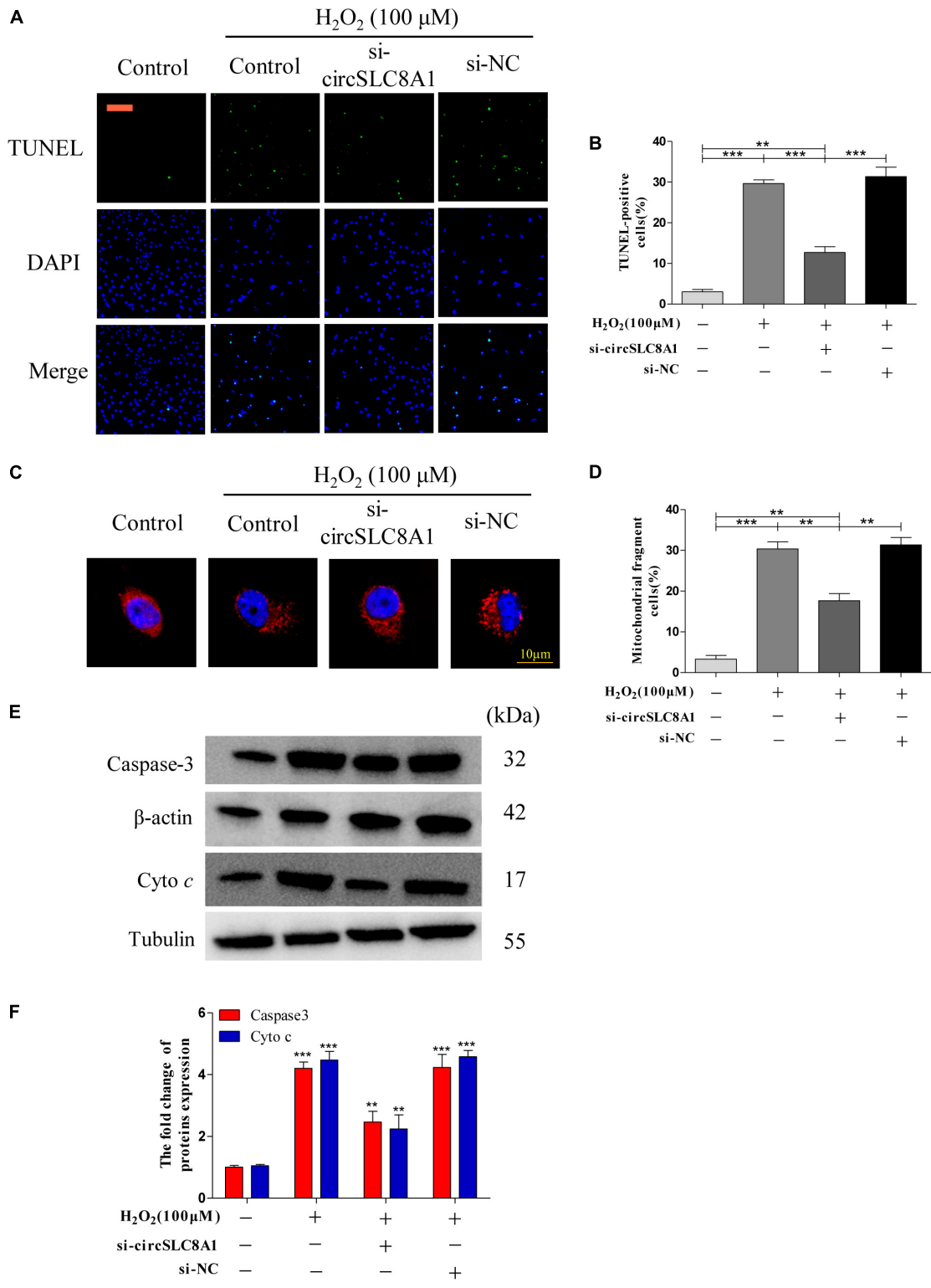


FIGURE 8 | Knockdown circSLC8A1 reduced myocardial cell to apoptosis under oxidative stress. **(A)** AC16 cells were exposed to 100 μM H₂O₂ for another 12 h after transfected with circSLC8A1-siRNA for 24 h, and apoptosis was stained with TUNEL. **(B)** The percentage of cells underwent TUNEL-positive cell. **(C)** AC16 cells were exposed to 100 μM H₂O₂ for another 12 h after the knockdown of circSLC8A1 expression, and the mitochondria was stained with MitoTracker Red. **(D)** The percentage of cells underwent mitochondrial fission. **(E)** The expression levels of apoptotic-related proteins were detected by western blotting. **(F)** The data analysis of blot densitometry. All the data were expressed as the mean ± SEM of three independent experiments. **P* < 0.05, ***P* < 0.01, ****P* < 0.001.

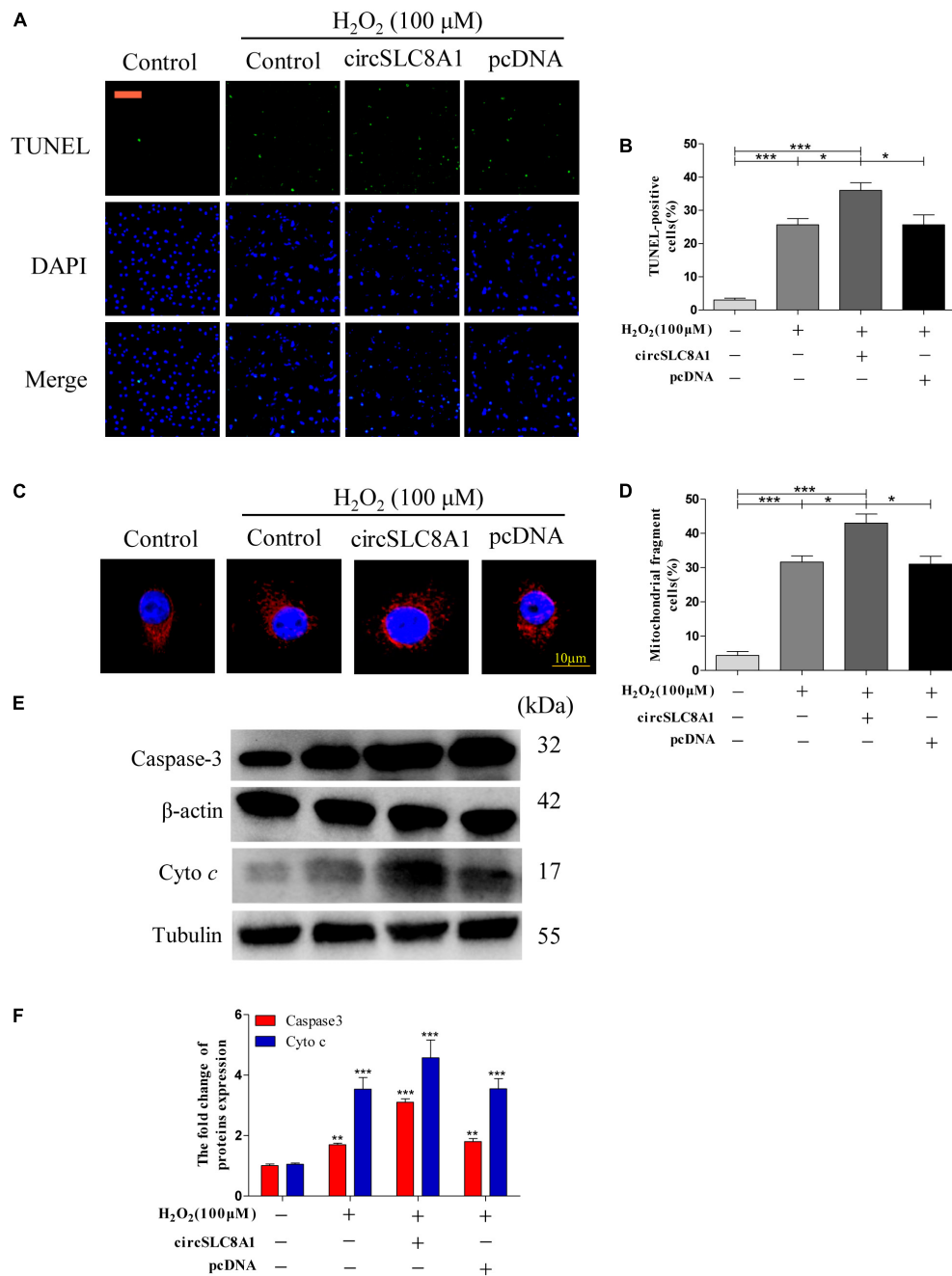


FIGURE 9 | Overexpression of circSLC8A1 sensitized myocardial cell to apoptosis under oxidative stress. **(A)** AC16 cells were exposed to 100 μM H₂O₂ for another 12 h after transfected with circSLC8A1-cDNA for 24 h, and apoptosis was stained with TUNEL. **(B)** The percentage of cells underwent TUNEL positive cell. **(C)** AC16 cells were exposed to 100 μM H₂O₂ for another 12 h after the overexpression of circSLC8A1, and the mitochondria was stained with MitoTracker Red. **(D)** The percentage of cells underwent mitochondrial fission. **(E)** The expression levels of apoptotic-related proteins were detected by western blotting. **(F)** The data analysis of blot densitometry. All of the data were expressed as the mean ± SEM of three independent experiments. **P* < 0.05, ***P* < 0.01, ****P* < 0.001.

circTMEM165, circUBAC2, circZNF609, circANKRD12, and circSLC8A1 in the peripheral blood of patients with MI. We observed the possible target mRNAs of these circRNAs including GREM1, WDR7, MYLK, ACSM2A, and RNF213. Moreover, the predicted target mRNAs played a key role in regulating organogenesis, body patterning, tissue differentiation, LDL

metabolism, and myosin interaction with actin, mitochondrial acyl-coenzyme A synthetase, and ATPase activity, respectively. All of them are highly correlated with CVDs.

To further clarify the potential mechanism of circSLC8A1 in MI, we tested the cell function through knockdown and overexpressed circSLC8A1 based on the cell model.

Uncontrolled mitochondrial fission contributes to apoptosis (39), which promotes the development of heart injury. Our results indicated that the knockdown of circSLC8A1 could maintain mitochondrial homeostasis and hence prevent the occurrence of apoptosis. Further experimental studies are needed to prove the specific signaling pathway.

A few limitations of this study ought to be mentioned. First, we only verified 10 circRNAs that were upregulated in MI, and still, a lot of differentially expressed circRNA needed to be verified. Second, although we use a set of filter methods to get the more accurate results, the sample size of this study is still limited, which will increase the false positive rate while analyzing RNASeq data. Third, we only explore more upregulated circRNAs, and the downregulated circRNAs are also worth studying in depth. Moreover, further experiments are needed to explore the regulatory effects of circRNAs in the occurrence of MI in patients with CVD.

CONCLUSION

To the best of our knowledge, this study is the first to report the expression profiles of circular RNA in the peripheral blood of patients with MI compared with healthy individuals. Bioinformatics analysis indicated that the upregulated expressions of circTMEM165, circUBAC2, circZNF609, circANKRD12, and circSLC8A1 were highly correlated with MI. Moreover, all of these five circRNAs may be used to improve the diagnosis accuracy of MI. Besides, the bioinformatics analysis found that these circRNAs could be involved in the regulation of hundreds of mRNAs, and numerous of these mRNAs may affect the occurrence of MI. Although our results revealed that these circRNAs are highly expressed in the peripheral blood of patients with MI, their predicted functions still need to be confirmed by further experiments.

DATA AVAILABILITY STATEMENT

The original contributions presented in the study are included in the article/**Supplementary Material**, further inquiries can be directed to the corresponding authors.

REFERENCES

1. WHO. *Cardiovascular Diseases (CVDs)*. (2017). Available online at: [https://www.who.int/news-room/fact-sheets/detail/cardiovascular-diseases-\(cvds\)](https://www.who.int/news-room/fact-sheets/detail/cardiovascular-diseases-(cvds)) (accessed on June 11, 2021).
2. Anderson JL, Morrow DA. Acute myocardial infarction. *N Engl J Med*. (2017) 376:2053–64.
3. Townsend N, Wilson L, Bhatnagar P, Wickramasinghe K, Rayner M, Nichols M. Cardiovascular disease in Europe 2016: an epidemiological update. *Eur Heart J*. (2016) 37:3182–3.
4. Kontou P, Pavlopoulou A, Braliou G, Bogiatzi S, Dimou N, Bangalore S, et al. Identification of gene expression profiles in myocardial infarction: a systematic review and meta-analysis. *BMC Med Genomics*. (2018) 11:109. doi: 10.1186/s12920-018-0427-x
5. Wu D, Zhang K, Hu P. The role of autophagy in acute myocardial infarction. *Front Pharmacol*. (2019) 10:551.
6. Swirski FK, Nahrendorf M. Cardioimmunology: the immune system in cardiac homeostasis and disease. *Nat Rev Immunology*. (2018) 18:733–44. doi: 10.1038/s41577-018-0065-8
7. Gabriel-Costa D. The pathophysiology of myocardial infarction-induced heart failure. *Pathophysiology*. (2018) 25:277–84. doi: 10.1016/j.pathophys.2018.04.003
8. Bougouin W, Marijon E, Puymirat E, Defaye P, Celermajer DS, Le Heuzey JY, et al. Incidence of sudden cardiac death after ventricular fibrillation complicating acute myocardial infarction: a 5-year cause-of-death analysis of the FAST-MI 2005 registry. *Eur Heart J*. (2014) 35:116–22.
9. Li M, Ding W, Tariq MA, Chang W, Zhang X, Xu W, et al. A circular transcript of ncx1 gene mediates ischemic myocardial injury by targeting miR-133a-3p. *Theranostics*. (2018) 8:5855–69. doi: 10.7150/thno.27285
10. Gyongyosi M, Winkler J, Ramos I, Do QT, Firat H, McDonald K, et al. Myocardial fibrosis: biomedical research from bench to bedside. *Eur J Heart Failure*. (2017) 19:177–91. doi: 10.1002/ehf.696

ETHICS STATEMENT

The studies involving human participants were reviewed and approved by Ethics Committee of Affiliated Hospital of Qingdao University. The patients/participants provided their written informed consent to participate in this study.

AUTHOR CONTRIBUTIONS

QL, JW, and YG conceived and designed the experiments. QL, YW, and YA collected and analyzed the data. QL and YW wrote this manuscript. All authors read and approved the final manuscript.

FUNDING

This study was supported by the National Science Foundation of China (grant number 81071246), and the Qingdao Minsheng Science and Technology Plan Project (grant number 18-6-1-80-nsh).

ACKNOWLEDGMENTS

We are grateful for the invaluable support and useful discussions with other members of the School of Basic Medical Sciences. The Department of Cardiology, Affiliated Hospital of Qingdao University supported this study.

SUPPLEMENTARY MATERIAL

The Supplementary Material for this article can be found online at: <https://www.frontiersin.org/articles/10.3389/fcvm.2022.810257/full#supplementary-material>

Supplementary Figure 1 | circRNA screening. Totally 5 circRNAs were screened out after comparison of our results with human heart tissue sequencing results.

Supplementary Figure 2 | ROC curve validation; 30% of the random sample was used to verify the ROC curve reliability of our data trained.

11. Ezekowitz JA, Kaul P, Bakal JA, Armstrong PW, Welsh RC, McAlister FA. Declining in-hospital mortality and increasing heart failure incidence in elderly patients with first myocardial infarction. *J Am Coll Cardiol.* (2009) 53:13–20.
12. Hsiao KY, Sun HS, Tsai SJ. Circular RNA – new member of noncoding RNA with novel functions. *Exp Biol Med.* (2017) 242:1136–41. doi: 10.1177/1535370217708978
13. Jens M. *Dissecting Regulatory Interactions of RNA and Protein.* Heidelberg: Springer Theses (2014). p. 69–80.
14. Sanger HL, Klotz G, Riesner D, Gross HJ, Ak K. Viroids are single-stranded covalently closed circular RNA molecules existing as highly base-paired rod-like structures. *Proc Natl Acad Sci U S A.* (1976) 73:3852–6. doi: 10.1073/pnas.73.11.3852
15. Ashwal-Fluss R, Meyer M, Pamudurti NR, Ivanov A, Bartok O, Hanan M, et al. circRNA biogenesis competes with pre-mRNA splicing. *Mol Cell.* (2014) 56:55–66. doi: 10.1016/j.molcel.2014.08.019
16. Li Z, Huang C, Bao C, Chen L, Lin M, Wang X, et al. Exon-intron circular RNAs regulate transcription in the nucleus. *Nat Struct Mol Biol.* (2015) 22:256–64.
17. Du WW, Fang L, Yang W, Wu N, Awan FM, Yang Z, et al. Induction of tumor apoptosis through a circular RNA enhancing Foxo3 activity. *Cell Death Differ.* (2017) 24:357–70. doi: 10.1038/cdd.2016.133
18. Cai L, Qi B, Wu X, Peng S, Zhou G, Wei Y, et al. Circular RNA Ttc3 regulates cardiac function after myocardial infarction by sponging miR-15b. *J Mol Cell Cardiol.* (2019) 130:10–22. doi: 10.1016/j.yjmcc.2019.03.007
19. Wang K, Long B, Liu F, Wang JX, Liu CY, Zhao B, et al. A circular RNA protects the heart from pathological hypertrophy and heart failure by targeting miR-223. *Eur Heart J.* (2016) 37:2602–11. doi: 10.1093/eurheartj/ehv713
20. Holdt LM, Stahringer A, Sass K, Pichler G, Kulak NA, Wilfert W, et al. Circular non-coding RNA ANRIL modulates ribosomal RNA maturation and atherosclerosis in humans. *Nat Commun.* (2016) 7:12429. doi: 10.1038/ncomms12429
21. Lei B, Zhou J, Xuan X, Tian Z, Zhang M, Gao W, et al. Circular RNA expression profiles of peripheral blood mononuclear cells in hepatocellular carcinoma patients by sequence analysis. *Cancer Med.* (2019) 8:1423–33. doi: 10.1002/cam4.2010
22. Langmead B, Trapnell C, Pop M, Salzberg SL. Ultrafast and memory-efficient alignment of short DNA sequences to the human genome. *Genome Biol.* (2009) 10:R25. doi: 10.1186/gb-2009-10-3-r25
23. Memczak S, Jens M, Elefsinioti A, Torti F, Krueger J, Rybak A, et al. Circular RNAs are a large class of animal RNAs with regulatory potency. *Nature.* (2013) 495:333–8. doi: 10.1038/nature11928
24. Gao Y, Zhang J, Zhao F. Circular RNA identification based on multiple seed matching. *Briefings Bioinform.* (2018) 19:803–10. doi: 10.1093/bib/bbx014
25. Liu XX, Yang YE, Liu X, Zhang MY, Li R, Yin YH, et al. A two-circular RNA signature as a noninvasive diagnostic biomarker for lung adenocarcinoma. *J Transl Med.* (2019) 17:50. doi: 10.1186/s12967-019-1800-z
26. Young MD, Wakefield MJ, Smyth GK, Oshlack A. Gene ontology analysis for RNA-seq: accounting for selection bias. *Genome Biol.* (2010) 11:R14. doi: 10.1186/gb-2010-11-2-r14
27. Kanehisa M, Araki M, Goto S, Hattori M, Hirakawa M, Itoh M, et al. KEGG for linking genomes to life and the environment. *Nucleic Acids Res.* (2008) 36:D480–4. doi: 10.1093/nar/gkm882
28. Mao X, Cai T, Olyarchuk JG, Wei L. Automated genome annotation and pathway identification using the KEGG orthology (KO) as a controlled vocabulary. *Bioinformatics.* (2005) 21:3787–93. doi: 10.1093/bioinformatics/bti430
29. Medina V, Edmonds B, Young GP, James R, Appleton S, Zalewski PD. Induction of caspase-3 protease activity and apoptosis by butyrate and trichostatin A (inhibitors of histone deacetylase): dependence on protein synthesis and synergy with a mitochondrial/cytochrome c-dependent pathway. *Cancer Res.* (1997) 57:3697–707.
30. Wang H, Ge W, Jiang W, Li D, Ju X. SRPK1-siRNA suppresses K562 cell growth and induces apoptosis via the PARP-caspase3 pathway. *Mol Med Rep.* (2018) 17:2070–6. doi: 10.3892/mmr.2017.8032
31. Werfel S, Nothjunge S, Schwarzmayr T, Strom TM, Meitinger T, Engelhardt S. Characterization of circular RNAs in human, mouse and rat hearts. *J Mol Cell Cardiol.* (2016) 98:103–7. doi: 10.1016/j.yjmcc.2016.07.007
32. Jeck WR, Sharpless NE. Detecting and characterizing circular RNAs. *Nat Biotechnol.* (2014) 32:453–61.
33. Jeck WR, Sorrentino JA, Wang K, Slevin MK, Burd CE, Liu J, et al. Circular RNAs are abundant, conserved, and associated with ALU repeats. *RNA.* (2013) 19:141–57. doi: 10.1261/rna.035667.112
34. Meng S, Zhou H, Feng Z, Xu Z, Tang Y, Li P, et al. CircRNA: functions and properties of a novel potential biomarker for cancer. *Mol Cancer.* (2017) 16:94. doi: 10.1186/s12943-017-0663-2
35. Li X, Wang Y, Han C, Li P, Zhang H. Colorectal cancer progression is associated with accumulation of Th17 lymphocytes in tumor tissues and increased serum levels of interleukin-6. *Tohoku J Exp Med.* (2014) 233:175–82. doi: 10.1620/tjem.233.175
36. Zhao T, Zheng Y, Hao D, Jin X, Luo Q, Guo Y, et al. Blood circRNAs as biomarkers for the diagnosis of community-acquired pneumonia. *J Cell Biochem.* (2019) 120:16483–94. doi: 10.1002/jcb.28863
37. Wu J, Zhou Q, Niu Y, Chen J, Zhu Y, Ye S, et al. Aberrant expression of serum circANRIL and hsa_circ_0123996 in children with Kawasaki disease. *J Clin Lab Anal.* (2019) 33:e22874. doi: 10.1002/jcla.22874
38. Wang L, Shen C, Wang Y, Zou T, Zhu H, Lu X, et al. Identification of circular RNA Hsa_circ_0001879 and Hsa_circ_0004104 as novel biomarkers for coronary artery disease. *Atherosclerosis.* (2019) 286:88–96. doi: 10.1016/j.atherosclerosis.2019.05.006
39. Guo M, Wang Y, Zhao H, Mu M, Yang X, Fei D, et al. Oxidative damage under As(3+) and/or Cu(2+) stress leads to apoptosis and autophagy and may be cross-talking with mitochondrial disorders in bursa of Fabricius. *J Inorg Biochem.* (2020) 205:110989. doi: 10.1016/j.jinorgbio.2019.110989

Conflict of Interest: The authors declare that the research was conducted in the absence of any commercial or financial relationships that could be construed as a potential conflict of interest.

Publisher's Note: All claims expressed in this article are solely those of the authors and do not necessarily represent those of their affiliated organizations, or those of the publisher, the editors and the reviewers. Any product that may be evaluated in this article, or claim that may be made by its manufacturer, is not guaranteed or endorsed by the publisher.

Copyright © 2022 Li, Wang, An, Wang and Gao. This is an open-access article distributed under the terms of the Creative Commons Attribution License (CC BY). The use, distribution or reproduction in other forums is permitted, provided the original author(s) and the copyright owner(s) are credited and that the original publication in this journal is cited, in accordance with accepted academic practice. No use, distribution or reproduction is permitted which does not comply with these terms.